CHEMICAL ENGINEERING TRANSACTIONS
VOL. 99, 2023
A publication of AIDIC
The Italian Association of Chemical Engineering
Online at www.cetjournal.it
Guest Editors: Sauro Pierucci, Flavio Manenti

ISBN 978-88-95608-98-3; **ISSN** 2283-9216
DOI: 10.3303/CET2399044

Photocatalytic Degradation of Phenol using Visible light Activated Ag-AgBr-Hydrotalcite Composite

Lehlogonolo S. Tabana*, Shepherd M. Tichapondwa

Department of Chemical Engineering, Sustainable Environmental and Water Utilisation Processes Division, University of Pretoria, Pretoria, South Africa.
tabana.ls@tuks.co.za

Water pollution is one of the persistent environmental challenges that continues to impact numerous communities worldwide. As such, several sustainable remediation technologies have been developed over the years to increase water supply through reuse. Visible light activated photocatalysis is one such technology that aptly remediates refractory organic pollutants from various water matrices. In this study, a composite Ag-AgBr-LDH photocatalyst was synthesized. The physical and chemical properties of the catalyst were elucidated using a range of characterization techniques. The photocatalytic activity of the material was tested on simulated phenol contaminated water, and degradation efficiencies as high as 92% were achieved at neutral pH and a catalyst loading of 2 g/L. The synthesized photocatalyst nanocomposite material proved to be a feasible catalyst for degradation of phenolic contaminants in water under visible light irradiation.

1. Introduction

Wastewater generated from industrial processes and agricultural activities contains toxic aromatic organic compounds (Mancipe et al., 2016). The presence of these phenolic compounds is associated with a multiplicity of health concerns due to their bio-recalcitrant nature which leads to bioaccumulation in aquatic species and humans. These contaminants are classified as endocrine-disrupting compounds and have known mutagenic and carcinogenic properties. It has been established that conventional bio-remediation processes are inadequate in degrading these refractory contaminants (Raza et al., 2019). This has led to the use of advanced oxidation processes (AOPs) as they are deemed to be cost effective and exhibit fast and non-selective oxidation reaction rates. Although several AOPs exist, heterogeneous photocatalysis is regarded as one of the most viable processes due to its ability to achieve higher degradation efficiencies, being eco-friendly and can be operated with ease (Chen et al., 2019).

Semiconductors, such as titanium dioxide (TiO_2), zinc oxide (ZnO) and ferric oxide (Fe_2O_3) have been reported to be effective photocatalysts for the oxidation and complete mineralization of pharmaceutical compounds, dyes, and a range of other phenolic compounds (Ahmed and Haider, 2018). Their photoactivity is driven by the formation of electron-hole pairs that are generated when the semiconductor is irradiated by a light source that emits energy greater or equal to the corresponding band gaps. Subsequently, the photo-generated holes can react with surface water molecules or hydroxyl ions (OH^-) to form ($^\bullet OH$) radicals that are known to be good oxidizing agents. While the electrons react with dissolved oxygen to form superoxide ($^\bullet O_2$) free radicals that have a slightly lower oxidizing potential compared to the hydroxyl radicals. Most semiconductors materials have wide band gaps that limit their activation to the UV light sources. As a result, a significant amount of energy is required to supply constant UV light irradiation and the lamps tend to be less effective over time and need frequent replacement. A potential solution to these limitations is the development of visible light activated photocatalysts that work under solar irradiation.

Layered double hydroxides (LDHs) clays are some of the materials with greater potential as photocatalysts in degradation of various organic pollutants. This is due to their appealing physicochemical properties that include adjustable structures and compositions, and higher specific areas. Studies on composite materials involving semiconductors and LDH clays have revealed that such materials offer better photodegradation efficiencies

Paper Received: 15 February 2023; Revised: 19 March 2023; Accepted: 19 April 2023
Please cite this article as: Tabana L.S., Tichapondwa S.M., 2023, Photocatalytic Degradation of Phenol using Visible light Activated Ag-AgBr-Hydrotalcite Composite, Chemical Engineering Transactions, 99, 259-264 DOI:10.3303/CET2399044

than the individual materials. The improved efficiencies on the composite materials are as a result of reduced turbidity and electron-hole pair recombination, increased adsorption capacities and inhibition of particle aggregation. Ternary LDH clays offer greater prospects in water remediation processes than binary LDH clays. This is due to the additional component enhancing the physicochemical properties of the material and ultimately improving its photocatalytic activity. In this study, an LDH clay containing of magnesium, zinc and aluminium was synthesized for application in photodegradation of phenol under visible light irradiation.
Silver halides (AgX where X represents Br, Cl, or I) have found applications in photocatalytic degradation processes owing to their activity upon visible light irradiation. Their utilization is limited due to photo corrosion caused by the deposits of metallic silver (Ag^0) on the surface of the photocatalyst and the prospects of high rate of electron-hole pair recombination. These shortfalls can be made less significant by coupling Ag-AgX with robust materials. This will enable Ag^0 nanoparticles to undergo surface plasmon resonance (SPR) phenomenon in order to absorb visible light photons.

2. Experimental

2.1 Materials

Aluminium, magnesium, and zinc chloride salts that were used for synthesis of LDH clay were sourced from Glassworld, South Africa. Silver nitrate ($AgNO_3$), Sodium bromide (NaBr), sodium hydroxide (NaOH) and phenol were procured from Merck. Acetonitrile, methanol, and hydrochloric acid (HCl) were supplied by Sigma Aldrich while acetic acid was received from Glassworld. Elga Purelab Flex 3 Water purifier was used for dispensation of deionized water that was used in all the experiments. The source of visible light irradiation was a 72 W LED lamb that had a peak wavelength range of 380 – 800 nm.

2.2 Synthesis of photocatalyst

Co-precipitation method was used to synthesize the LDH clay. This process was operated at a constant pH of 10 to supress the formation of metal hydroxides. The metal solutions contained molar ratios of Mg (75%), Zn (5%) and Al (20%). The synthesis was controlled at 60 ℃. A facile photo-assisted method was used for synthesis of the composite photocatalyst. 1 g of LDH clay was added to 200 mL of water and dispersed through ultrasonication for 45 min. Thereafter, 0.5 g Ag (added as $AgNO_3$) was dissolved in 5 mL of water and poured into the LDH clay suspension. This was mixed for 2 h prior to adding 20 mL of 2 M NaBr solution. The suspension was stirred in the dark for a further 2 h period. 20 mL of methanol was then added to the suspension and mixed for another hour. The resulting precipitate was recovered through centrifugation and washed 3 times with water and once with methanol. This photocatalyst was labelled LDH-doped 15. LDH-doped 7.5 and LDH-doped 30 were synthesized by varying the amount of Ag added. Ag-AgBr photocatalyst was synthesized using the same process without adding LDH clay.

2.3 Characterization of photocatalyst

The photocatalysts were characterized to establish their elemental composition, mineralogy, morphology, and BET surface area. X-ray powder diffraction (XRD) spectra were determined using a PANalytical X'Pert Pro powder diffractometer in θ-θ configuration fitted with an X'Celerator detector and variable divergence with Fe-filtered Co-Kα radiation (λ = 1.789 Å) fixed slits. Data was collected in the angular range of 5 to 90° 2θ with a step size of 0.008° 2θ and 13 s scan step time. The mineral phases present were confirmed using X'Pert Highscore plus software, which indexed the spectra against the ICSD database. A Zeiss Ultra Plus field emission scanning electron microscope (FEG-SEM) was used to capture the SEM/EDS images. SEM samples were prepared by distributing the samples on carbon tape stuck to a microscopy stub; the samples were then sputter coated with carbon under argon gas. A Micrometrics Tristar 3000 BET analyzer was used to determine the BET surface area. All samples were degassed for 24 hours at 150°C under a 10^{-5} Torr vacuum before analysis.

2.4 Photocatalytic degradation experiments

The photodegradation tests were conducted in a closed compartment lined with a reflective material. Magnetic stirrers were kept in the compartment for mixing with sources of irradiation placed directly above the mixers. 100 mL of phenol solution was used in all the experiments. The effect of Ag content was evaluated by using photocatalysts with varying Ag content. The effect of photocatalyst loading was assessed by varying the catalyst loading between 0 to 4 g/L. pH evaluated ranged from 5 to 12 while the effect of initial concentration was tested at 5, 10 and 20 mg/L. reusability studies were conducted by recovering the spent photocatalyst after each experimental run, wash and dry it before reusing in the proceeding runs. In all the experiments, phenol-catalyst suspensions were allowed to mix and equilibrate in the dark for 30 min prior to illumination. Samples were withdrawn at predetermined periods, filtered, and analyzed through high performance liquid chromatography

(HPLC). A Waters 2695 HPLC coupled with a Waters 2489 UV-vis detector was used for analyses. The mobile phase of the HPLC was made of 70% acetonitrile and 30% water with both solvents containing 0.1% acetic acid.

3. Results and discussion

3.1 Phase identification and morphology of photocatalysts

The phases of the photocatalysts were determined through XRD analysis (Figure 1). The regular LDH peaks were identified thereby indicating the success in synthesis of the clay. The composite photocatalyst was successfully synthesized as its XRD analysis displayed the characteristics peaks of both LDH clay and Ag-AgBr. Furthermore, the formation of metallic silver was confirmed by the presence of a feint Ag peak. Figure 2 shows the morphologies of the photocatalysts. Figure 2(a) displays the platelet structures associated with hydrotalcites. Figure 2(b) shows the spherical particles that are synonymous with Ag-AgBr. Figure 2(c) and (d) show the platelet structures covered by the spherical structures to indicate the presence of both hydrotalcite and Ag-AgBr.

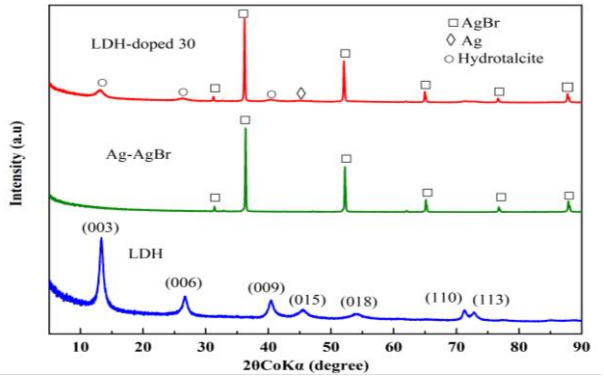

Figure 1: X-ray diffraction spectra of neat LDH, Ag-AgBr and LDH-doped 30 composite catalysts

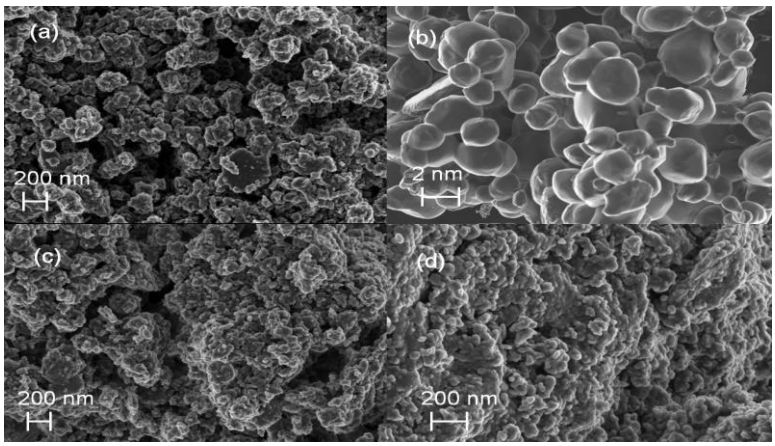

Figure 2: SEM analysis (a) LDH, (b) Ag-AgBr, (c) LDH-doped 15, and (d) LDH-doped 30

3.2 Photocatalytic performance study

3.2.1 Effect of Silver content

Figure 3 shows the degradation efficiencies of phenol with varied compositions of Ag in the photocatalysts. The pristine LDH adsorbed 4% phenol in the dark while the photodegradation control experiment resulted in 19% degradation efficiency under visible light irradiation. Previous studies show similar findings under adsorption conditions (Tabana et al., 2020) and photolysis (Gevers et al., 2022). The photocatalyst containing only Ag and AgBr was able to reach 8 and 45% phenol degradation in the dark and under visible light irradiation respectively. Doped clay materials showed an improvement in phenol degradation efficiencies in comparison with the neat clay. There was a slight increase in degradation efficiency (52 to 57%) when the Ag content in the photocatalyst composite was increased from 0.075 to 0.15 g per 1 g of LDH after 8 h of visible light irradiation. Phenol removal of 76% was observed when 0.3 g Ag per 1 g LDH was used

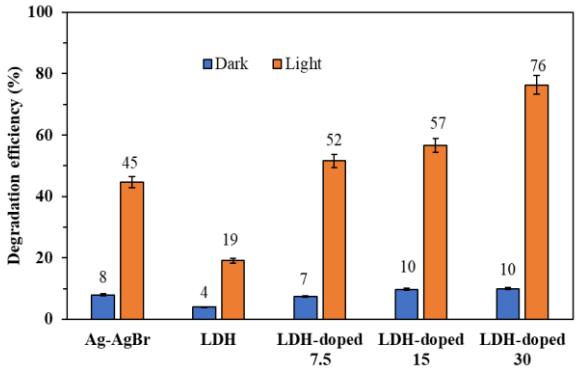

Figure 3: Phenol degradation efficiencies with varying Ag content in the photocatalyst

3.2.2 Effect of catalyst loading

Figure 4 shows how the degradation efficiency varied with catalyst dosage from photolysis (0 g/L) to 4 g/L. Phenol degradation efficiency increased with catalyst loading up to 2 g/L with the highest removal of 92% observed after 8 h. An increase in photocatalyst loading beyond 2 g/L (at 4 g/L) resulted in an increase in solution turbidity and subsequently a decrease in photocatalytic degradation of phenol. An increase in the amount of photocatalyst is expected to increase the photocatalytic efficiency, as more active sites become available. However, excess amount of nanoparticles in a photocatalytic reactor can create a light screening effect that can lead to a reduction in surface area of the nanoparticles being exposed to light; this will subsequently affect the photocatalytic efficiency.

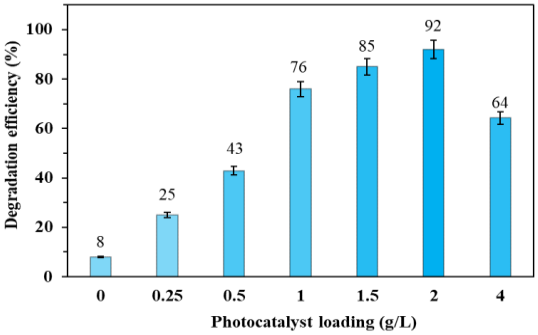

Figure 4: Phenol degradation efficiencies with varying photocatalyst loading

3.2.3 Effect of pH

Figure 5 shows the effect of pH on the extent of phenol degradation. The highest phenol degradation efficiency occurred when the initial pH of the solution was kept at 6.68 (unadjusted pH). Phenol adsorption capacities using LDH clays have been reported to be at their highest at neutral pH (Lupa et al., 2018). This is due to the hydrogen bonds between the surface of the photocatalyst and the hydroxyl groups in phenol. The degradation efficiencies of phenol in acidic and basic conditions were lower compared to neutral conditions due to the following reasons. In an acidic medium, phenol does not dissociate, which means that the solution would contain phenol, protons, and chloride ions. Chloride ions can inhibit photocatalysis degradation of phenol by acting as scavengers for photo-induced holes and hydroxyl radicals, as shown in Equation (1) and (2).

$$Cl^- + \bullet OH \rightarrow Cl + OH^- \quad (1)$$

$$Cl^- + h_{vb}^+ \rightarrow Cl\bullet \quad (2)$$

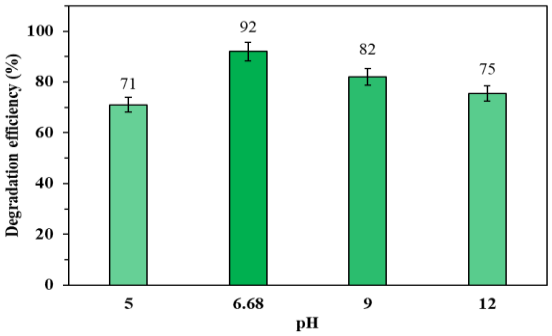

Figure 5: Effect of pH on phenol degradation efficiencies

3.3.4 Reaction kinetics and the effect of phenol concentration

An increase in phenol concentration from 5 mg/L to 10 mg/L led to a reduction in the extent of phenol degradation from 100% to 73% in 4 h (Figure 6). A further decline in phenol degradation efficiency from 73% to 44% was observed when the initial concentration was increased from 10 mg/L to 20 mg/L within the same period. The three possible reasons for the decline in degradation efficiency at elevated concentrations as elaborated by Li et. al. (2019) were firstly, the formation of intermediate products results in competition with the primary pollutant for active sites leading to poor contact between the pollutant and photocatalyst. Secondly, the generation of radicals on the surface is reduced in the presence of high pollutant concentration since the active sites are covered by pollutant molecules, and lastly a significant amount of light can be absorbed by pollutant leading to a drop in the generation of active radicals.

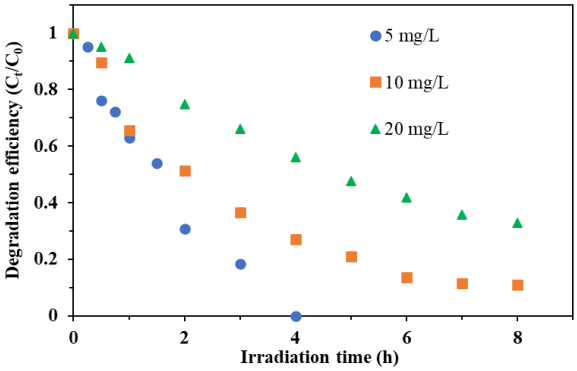

Figure 6: Phenol degradation efficiencies at various initial concentrations

The kinetics of photocatalytic reactions of organic contaminants are usually described by the Langmuir-Hinshelwood (L-H) model. The simplified L-H model is shown in Equation 3. Where C_0 is the initial concentration, C_t is the concentration at time t and k_{app} represents the apparent rate constant. The plot of $\ln(C_0/C_t)$ against irradiation time t is linear with k_{app} being the slope. Table 1 shows the parameters from the lineal plot of phenol degradation at various initial concentrations.

$$\ln\left(\frac{C_0}{C_t}\right) = k_{app}t \quad (3)$$

Table 1: Apparent rate constant, half-life, and linearization coefficient for the Langmuir-Hinshelwood model at various concentrations

Concentration (mg/L)	k_{app} (h^{-1})	($t_{1/2}$) (h)	R^2
5	0.578	1.32	0.978
10	0.294	2.12	0.985
20	0.146	4.86	0.997

3.3.5 Photo stability and reusability of the catalyst

The composite catalyst was recycled in a series of tests to evaluate its stability and reusability. Figure 7 shows a gradual decrease in the degradation efficiency after the first two cycles from 92% to 80% degradation. Thereafter there was 27% decrease in efficiency between Run 3 and 4. The drop in degradation efficiency could be caused by higher reduction of silver ions to form Ag^0. While Ag^0 plays a role in SPR phenomenon, it has a potential to cause photo-corrosion of the catalyst when present in elevated quantities. Therefore, it can be postulated that the increased amounts of Ag^0 caused photo-corrosion of the photocatalyst which resulted in a decline in degradation efficiency.

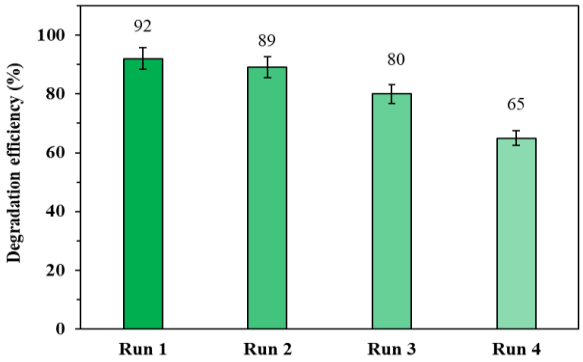

Figure 7: Stability and reusability tests of the photocatalyst

4. Conclusion

A photocatalyst containing Ag-AgBr and LDH clay was successfully synthesized through photo-induced reduction method. This composite proved to be more effective in degrading phenol than Ag-AgBr and LDH clay separately. The presence of Zn in the photocatalyst was vital in enhancing the photocatalytic activity of the material and subsequently led to a higher phenol degradation efficiency. More than 92% of phenol was degraded over 8 h at neutral pH, under visible light irradiation.

Acknowledgement

This research study was funded by the National Research Foundation (NRF) of South Africa (grant numbers:117905 and MND200409512185).

References

Ahmed S.N., Haider W., 2018, Heterogeneous photocatalysis and its potential applications in water and wastewater treatment: A review, Nanotechnology, 29, 342001.

Chen C.R., Zeng H.Y., Yi M.Y., Xiao G.F., Zhu R.L., Cao X.J., Shen S.G., Peng J.W., 2019, Fabrication of Ag2O/Ag decorated ZnAl-layered double hydroxide with enhanced visible light photocatalytic activity for tetracycline degradation, Ecotoxicology and Environmental Safety, 172, 423–431.

Gevers B.R., Roduner E., Labuschagné F.J., 2022, Towards understanding photon absorption and emission in MgAl layered double hydroxide, Material Advanced, 3, 962–977.

Li B., Lai C., Xu P., Zeng G., Huang D., Qin L., . . . F. Huang F., 2019, Facile synthesis of bismuth oxyhalogen-based z-scheme photocatalyst for visible-light-driven pollutant removal: Kinetics, degradation pathways and mechanism, Journal of Cleaner Production, 225, 898–912.

Lupa L., Cocheci L., Pode R., Hulka I., 2018, Phenol adsorption using aliquat 336 functionalized Zn-Al layered double hydroxide, Separation Purification Technology, 196, 82–95.

Mancipe S., Tzompantzi F., Rojas H., Gómez R., 2016, Photocatalytic degradation of phenol using MgAlSn hydrotalcite-like compounds, Applied Clay Science 129, 71–78.

Raza W., Kukkar D., Saulat H., Raza N., Azam M., Mehmood A., Kim K.H., 2019, Metal-organic frameworks as an emerging tool for sensing various targets in aqueous and biological media, TrAC Trends in Analytical Chemistry, 115654.

Tabana L., Tichapondwa S., Labuschagne F., Chirwa E., 2020, Adsorption of phenol from wastewater using calcined magnesium-zinc-aluminium layered double hydroxide clay, Sustainability, 12, 4273.